RSC Advances

PAPER

View Article Online
View Journal | View Issue

Cite this: *RSC Adv.*, 2021, **11**, 2141

Synthesis of biological based hennotannic acid-based salts over porous bismuth coordination polymer with phosphorous acid tags†

Saeed Babaee,[a] Mahmoud Zarei,[a]* Mohammad Ali Zolfigol,[a]* Sadegh Khazalpour,[b] Masoumeh Hasani,[b] Uwe Rinner,[c] Romana Schirhagl,[d] Neda Norouzi[d] and Sadegh Rostamnia[e]

Received 2nd August 2020
Accepted 20th November 2020

DOI: 10.1039/d0ra06674e

rsc.li/rsc-advances

In this paper, a novel porous polymer capable of coordinating to bismuth (PCPs-Bi) was synthesized. The Bi-PCPs was then reacted with phosphorous acid to produce a novel polymer PCPs(Bi)N$(CH_2PO_3H_2)_2$ which is shown to act as an efficient and recyclable catalyst. The mentioned catalyst was applied for the efficient synthesis of new mono and bis naphthoquinone-based salts of piperidine and/or piperazine *via* the reaction of hennotannic acid with various aldehydes, piperidine and/or piperazine, respectively. The structure of the resulting mono and bis substituted piperazine or piperidine-based naphthoquinone salts was thoroughly characterized spectroscopically. The electrochemical behavior of the products was also investigated. The presented protocol has the advantages of excellent yields (82–95%), short reaction times (4–30 min) and simple work-up.

1. Introduction

Nowadays, porous material frameworks such as porous coordination polymers (PCPs) and metal–organic frameworks (MOFs), a combination of organic ligands and metal, are commonly used in catalysts, adsorption, gas storage, *etc*[1–10]. To the best of our knowledge, most of the bismuth salts are safe and this metal is known to be non-toxic and stable.[11–14] Due to its high stability and non-toxicity it is used in cosmetics and pigments and has been used in equipment for drinking water. Additionally, it is added to multi-drug systems and as an alternative to lead in industry.[15,16] In addition, bismuth-based porous material frameworks have been used for fluorescence-based detection.[17] On the other hand, the emphasis of science and technology has shifted to design heterogeneous selective catalysts based on renewable, nanoporous, organic–inorganic hybrid and neutral materials. These often show lower toxicity and thus produce less hazardous waste. They are reusable, and have higher turnover numbers (TON) and turnover frequencies (TOF). In this regard, porous coordination polymers (PCPs) have been reported as porous catalysts which have high surface area and thermal stability.[18,19]

Phosphorus functional groups are essential linkers within the molecular structural of living cells and organisms.[20] Acidic phosphorous derivatives are made from mineral phosphorus derivatives, which are naturally found in the body. One of their calcium salts contributes to the formation of healthy bones and teeth.[21,22] These materials are a common additive for preserving flavors and bacteria in many foods processing routines.[23] It also plays an important role in photosynthesis, cell division, respiration and energy transfer.[24] Recently we have reported glycoluril, SBA-15, En/MIL-100(Cr) and melamine with phosphorous acid tags for the synthesis of organic compounds with biological properties.[25–28]

2-Hydroxynaphthalene-1,4-dione (hennotannic acid) or lawsone with a red-orange color is extracted from the leaves of the henna plant.[29] Henna is used for dyeing of skin, hair, fabrics, fingernails, silk, wool and leather. Lawsone has been also used for the preparation of azo dyes,[30] xanthenes and bis-coumarins,[31] chromene derivatives,[32] spirocompounds,[33] and leucodyes.[34]

Naphthoquinone derivatives are main constituents of the lawson interims (Hana) found in abundance in leaves and bark.[35] These structures have some medicinal and healing properties. They are antioxidant,[36] antibacterial,[37]

[a]*Department of Organic Chemistry, Faculty of Chemistry, Bu-Ali Sina University, PO Box 6517838683, Hamedan, Iran. E-mail: mahmoud8103@yahoo.com; zolfi@basu.ac.ir; mzolfigol@yahoo.com; saeed.babai@yahoo.com; Fax: +988138380709; Tel: +988138282807*

[b]*Department of Analytical Chemistry, Faculty of Chemistry, Bu-Ali Sina University, Hamedan, Iran. E-mail: khazalpour@yahoo.com; hasani@basu.ac.ir*

[c]*Department of Life Sciences, IMC University of Applied Sciences, Piaristengasse 1, 3500 Krems, Austria. E-mail: uwe.rinner@fh-krems.ac.at*

[d]*University Medical Center Groningen, Groningen University, Antonius Deusinglaan 1, 9713 AV Groningen, Netherlands. E-mail: romana.schirhagl@gmail.com; n.norouzi2018@gmail.com*

[e]*Organic and Nano Group (ONG), Department of Chemistry, Faculty of Science, University of Maragheh, PO Box 55181-83111, Maragheh, Iran. E-mail: rostamnia@maragheh.ac.ir*

† Electronic supplementary information (ESI) available. See DOI: 10.1039/d0ra06674e

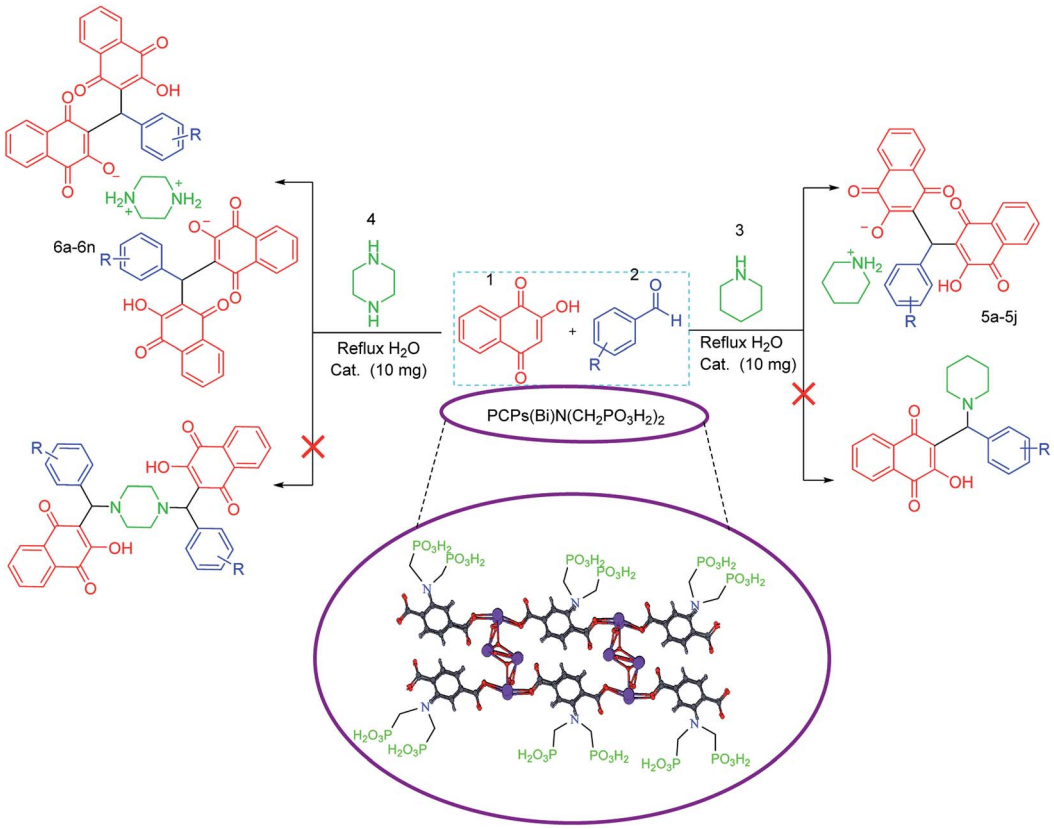

Scheme 1 Synthesis of mono and bis naphthoquinone based salts of piperidine and/or piperazine using $PCPs(Bi)N(CH_2PO_3H_2)_2$.

Table 1 Effect of different amounts of catalysts, temperature and solvent (5 mL) in the synthesis of naphthoquinone derivatives based on piperazine and piperidine

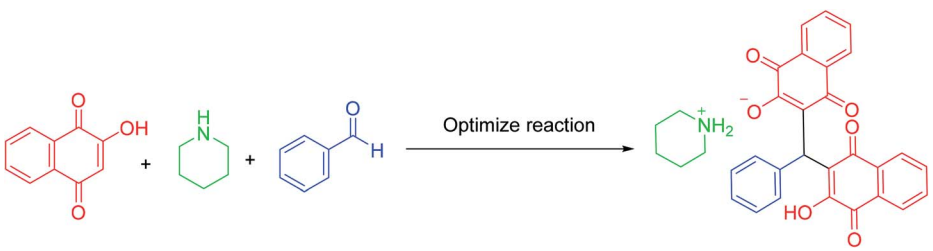

Entry	Catalyst (mg)	Temp. (°C)	Solvent	Time (min)	Yield (%)
1	—	Reflux	H_2O	90	Trace
2	1	Reflux	H_2O	60	35
3	3	Reflux	H_2O	45	50
4	5	Reflux	H_2O	33	57
5	7	Reflux	H_2O	15	78
6	**10**	**Reflux**	**H_2O**	**5**	**92**
7	15	Reflux	H_2O	5	92
8	10	80	H_2O	25	75
9	10	50	H_2O	40	45
10	10	Rt	H_2O	60	32
11	10	—	100	25	70
12	10	100	DMF	20	67
13	10	Reflux	EtOH	15	64
14	10	Reflux	$CHCl_3$	35	35
15	10	Reflux	EtOAc	30	58
16	10	Reflux	CH_3CN	20	60
17	10	Reflux	Toluene	90	Trace

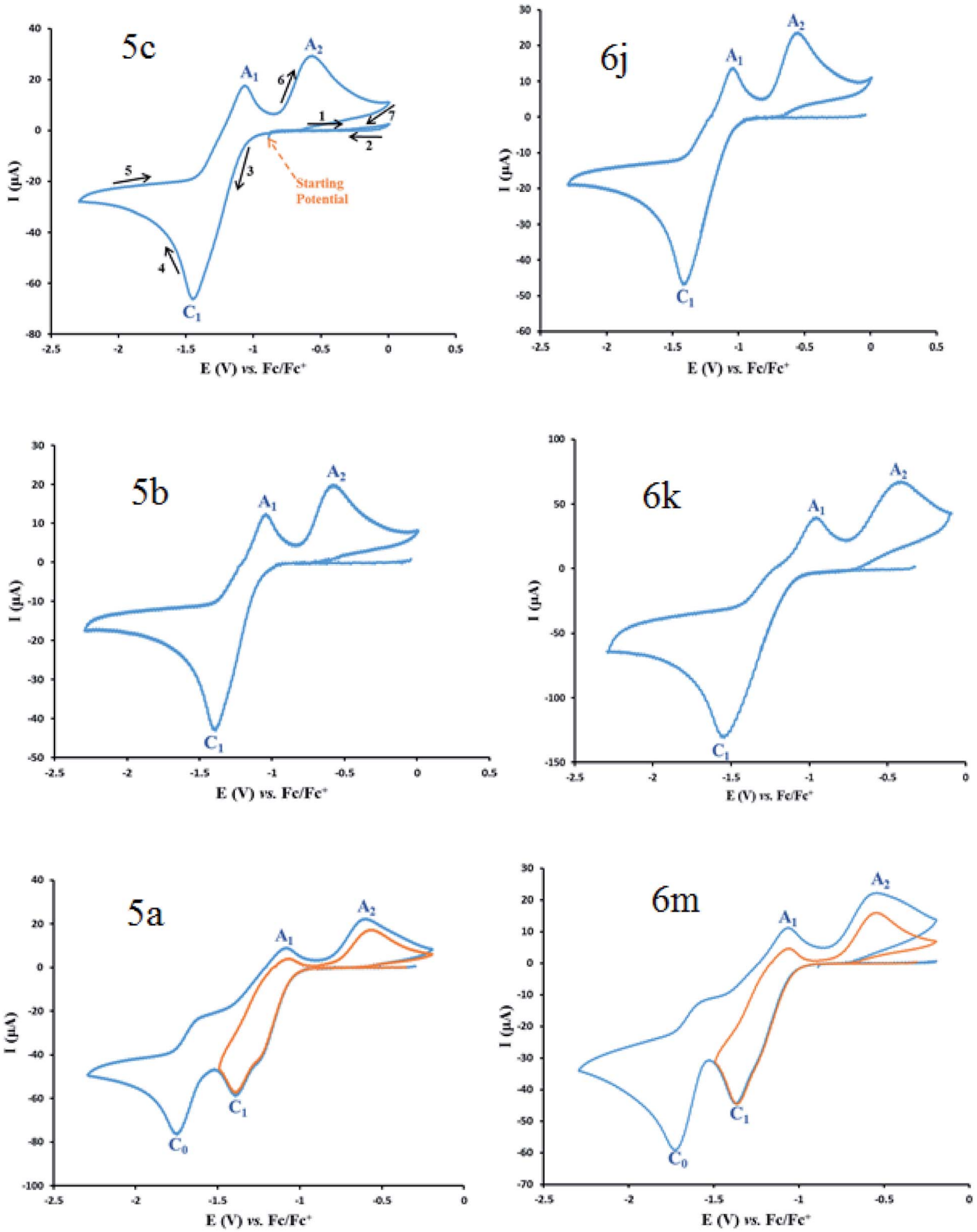

Fig. 1 Cyclic voltammograms of a saturated solution of the product (**5b**, **6k**, **5c**, **6j**, **5a** and **6m**) in DMSO containing tetra-*n*-butylammonium perchlorate (0.1 M), at glassy carbon electrode. Sweeping direction: oxidation of the obtained products at the first stage, reduction at the second stage and oxidation at the third stage. Scan rate: 100 mV s^{-1}. Temperature = 25 ± 1 °C. Vectors show the sweeping direction.

antifungal,[38,39] hepatoprotective,[39] anti-inflammatory,[40] antiviral, anticancer,[41] protein glycation inhibiting[42] and antiparasitic.[43] Very recently, we have studied the electrochemical reduction of lawsone based xanthenes *via* chronoamperometry, cyclic voltammetry, and differential pulse voltammetry at a glassy carbon electrode.[44] The above said properties have led to the synthesis of various naphthoquinone-based compounds which exhibited a variety of biological properties.[45,46]

Since that bismuth is the only one of that group to be non-toxic, we decided to apply it for synthesis of its corresponding porous coordination polymer with phosphorous acid tags. Therefore, herein, a novel porous coordination polymer containing bismuth (Bi) with phosphorous acid tags PCPs(Bi) $N(CH_2PO_3H_2)_2$ was synthesized. We used this material as a nano-porous catalyst for the synthesis of new naphthoquinone derivatives. Mono [piperidin-1-ium-1,4-dihydronaphthalen-2-olate] (**5a–5j**) and bis [piperazine-1,4-diium-1,4-dihydronaphthalen-2-olate] (**6a–6n**) henna-based salts of piperidine and/or piperazine were synthesized respectively, from the reaction of 2-hydroxynaphthalene-1,4-dione (henna), various aldehydes and piperazine or piperidine under reflux water condition (Scheme 1). As presented in the Scheme 1 the second reactions paths were not occurred.

2. Experimental

2.1. Materials and methods

The materials such as 2-aminoterephthalic acid (BDC-NH_2) (Sigma-Aldrich, 99%), bismuth(III) nitrate pentahydrate ($Bi(NO_3)\cdot 5H_2O$) (Merck, 95%), formic acid (HCOOH) (Merck, 37%), ethanol (C_2H_5OH) (Merck, 99%), lithium perchlorate ($LiClO_4$) (Merck, 99%), 2-hydroxynaphthalene-1,4-dione (Sigma-Aldrich, 99%), piperidine and piperazine (Sigma-Aldrich, 99%) and other materials (Merck) were reagent-grade materials and used as received without further purification.

2.2. Instrumental measurements

From the model of the BRUKER Ultrashield FT-NMR spectrometer (δ in ppm) were recorded ^{1}H NMR (600 or 400 MHz), ^{13}C NMR (151 or 101 MHz) ^{13}C NMR (DEPT-135), ^{1}H^{1}H Cosy, ^{1}H^{13}C HSQC, and ^{1}H^{13}C HMBC. Recorded on a Büchi B-545 apparatus in open capillary tubes were melting points. The PerkinElmer PE-1600-FTIR device was recorded for infrared spectra of compounds. SEM was performed using a scanning electron microscope for field publishing made by TE-SCAN. Thermal gravimetry (TG), differential thermal gravimetric (DTG) and differential thermal (DTA) were analyzed by a Perkin Elmer (Model: Pyris 1). BET and BJH were

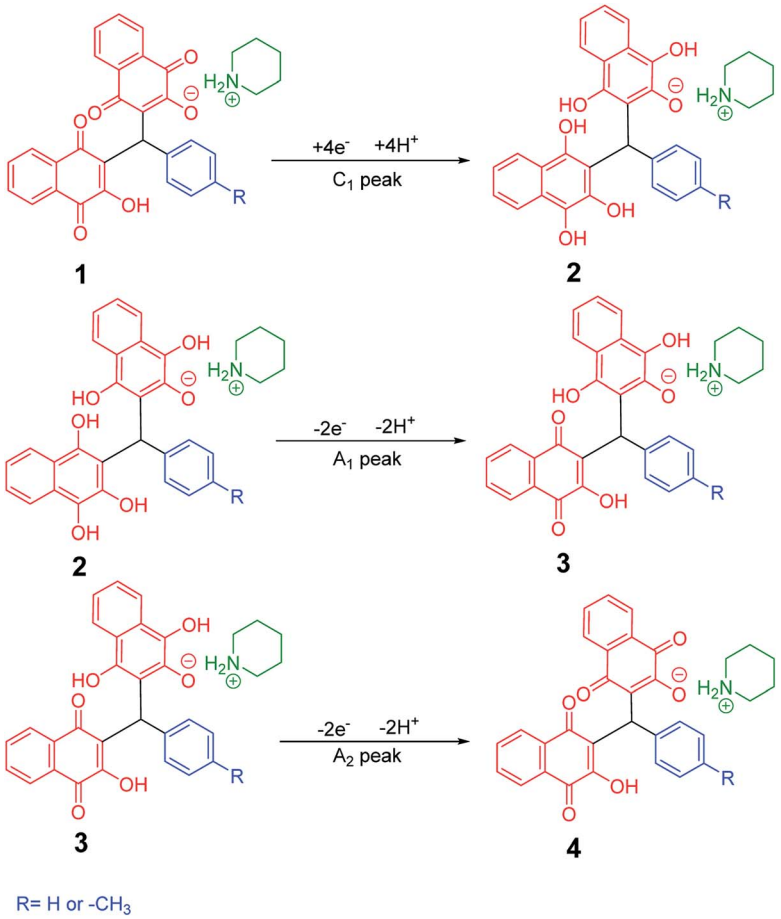

Scheme 2 Proposed mechanism of electrochemical process in **5b** and **5c** cyclic voltammograms in Fig. 1.

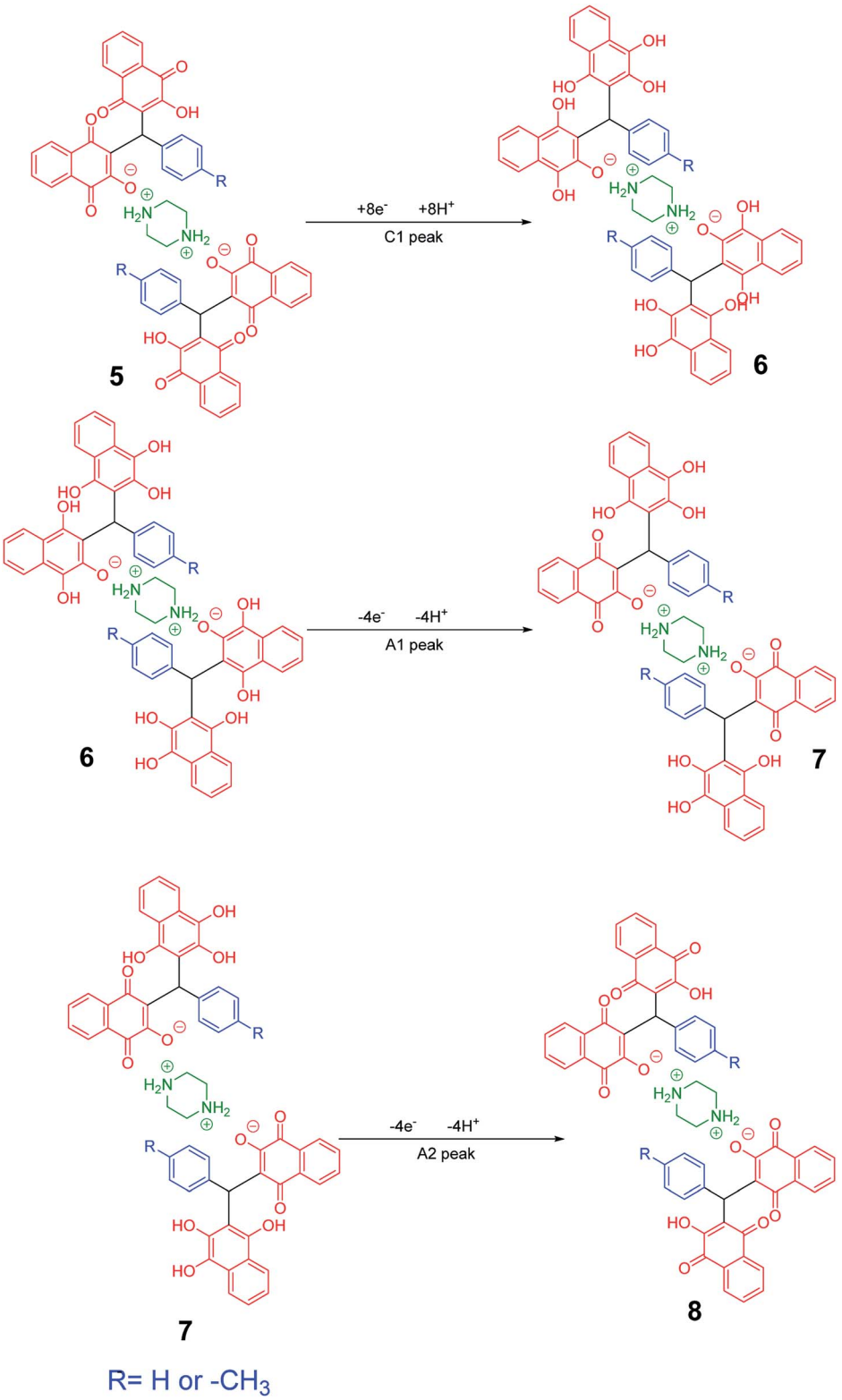

Scheme 3 Proposed mechanism of electrochemical process in **6k** and **6j** cyclic voltammograms in Fig. 1.

analyzed by BELSORP-mini ii high precision surface area and pore size. XRD was analyzed by ITAL STRUCTURE APD2000.

2.3. Electrochemical test

Cyclic voltammetry was performed using an Autolab model PGSTAT204 potentiostat/galvanostat. The working electrode used in the voltammetry experiments was a glassy carbon disc (3.2 mm^2 area) and a platinum wire was used as a counter electrode. An Ag wire electrode was used as a reference electrode for all experiments and all potential values were reported with reference to ferrocene/ferrocenium couple (Fc/Fc^+) as an internal standard. Tetrabutylammonium perchlorate was reagent-grade materials from Aldrich. Cyclic voltammetric measurements of each solution was carried out in a tetrabutylammonium perchlorate solution as the supporting electrolyte. A saturated solution of some product (**5b**, **6k**, **5c**, **6j**, **5a** and **6m**) and tetrabutylammonium perchlorate (0.1 M) in DMSO, was put into the voltammetric cell and was deoxygenated with high-purity nitrogen (99.999%) for about 25 min. The background voltammograms were obtained by scanning the potential from 1.00 V to about −2.2 V.[47]

2.4. Catalytic tests

The mentioned naphthoquinone compounds were synthesized in the presence of $PCPs(Bi)N(CH_2PO_3H_2)_2$ as catalyst *via* one-pot reaction of 2-hydroxynaphthalene-1,4-dione (4 mmol or 2 mmol), piperazine or piperidine (1 mmol), aryl aldehyde (2 mmol or 1 mmol). The condensation of 2-hydroxynaphthalene-1,4-dione (2 mmol, 0.348 g), piperidine (1 mmol, 0.085 g) and benzaldehyde (1 mmol, 0.106 g) was

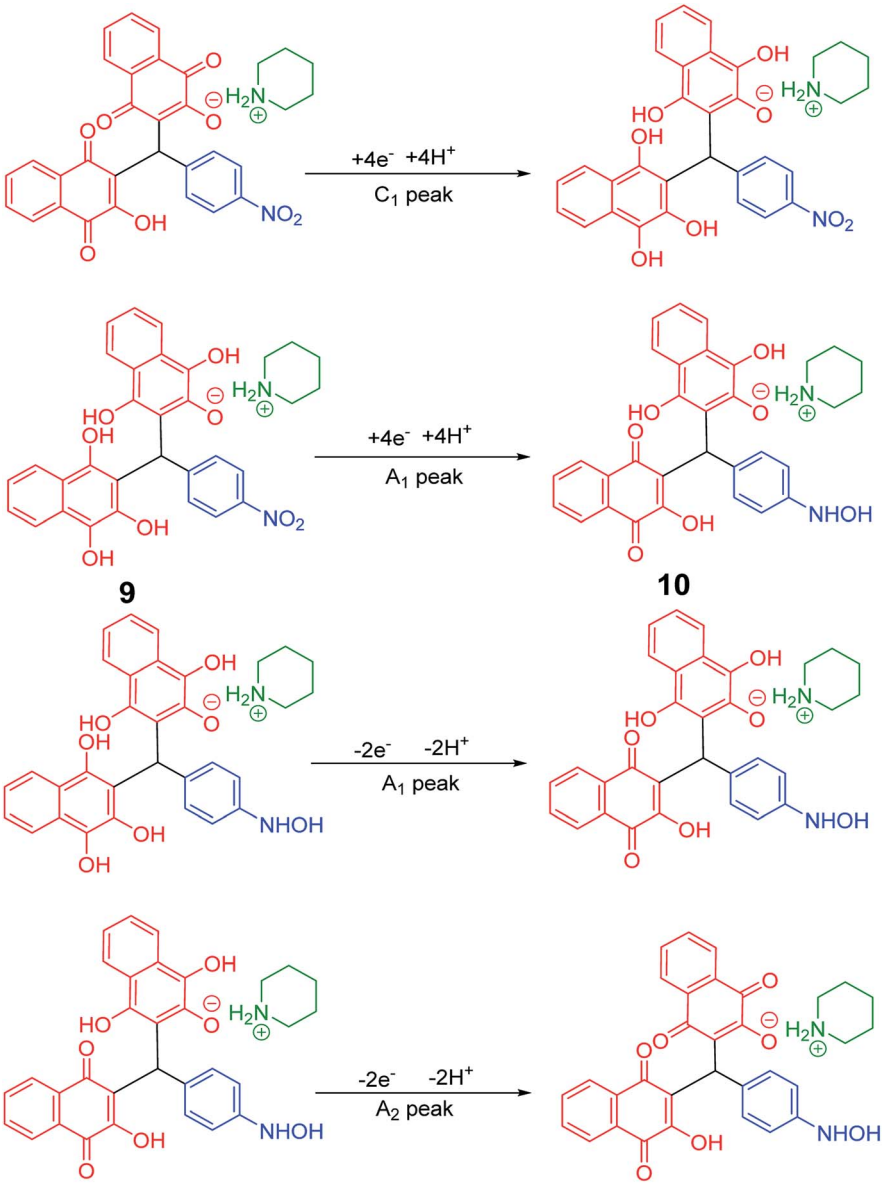

Scheme 4 Proposed mechanism of the electrochemical process of **5a** cyclic voltammogram in the Fig. 1.

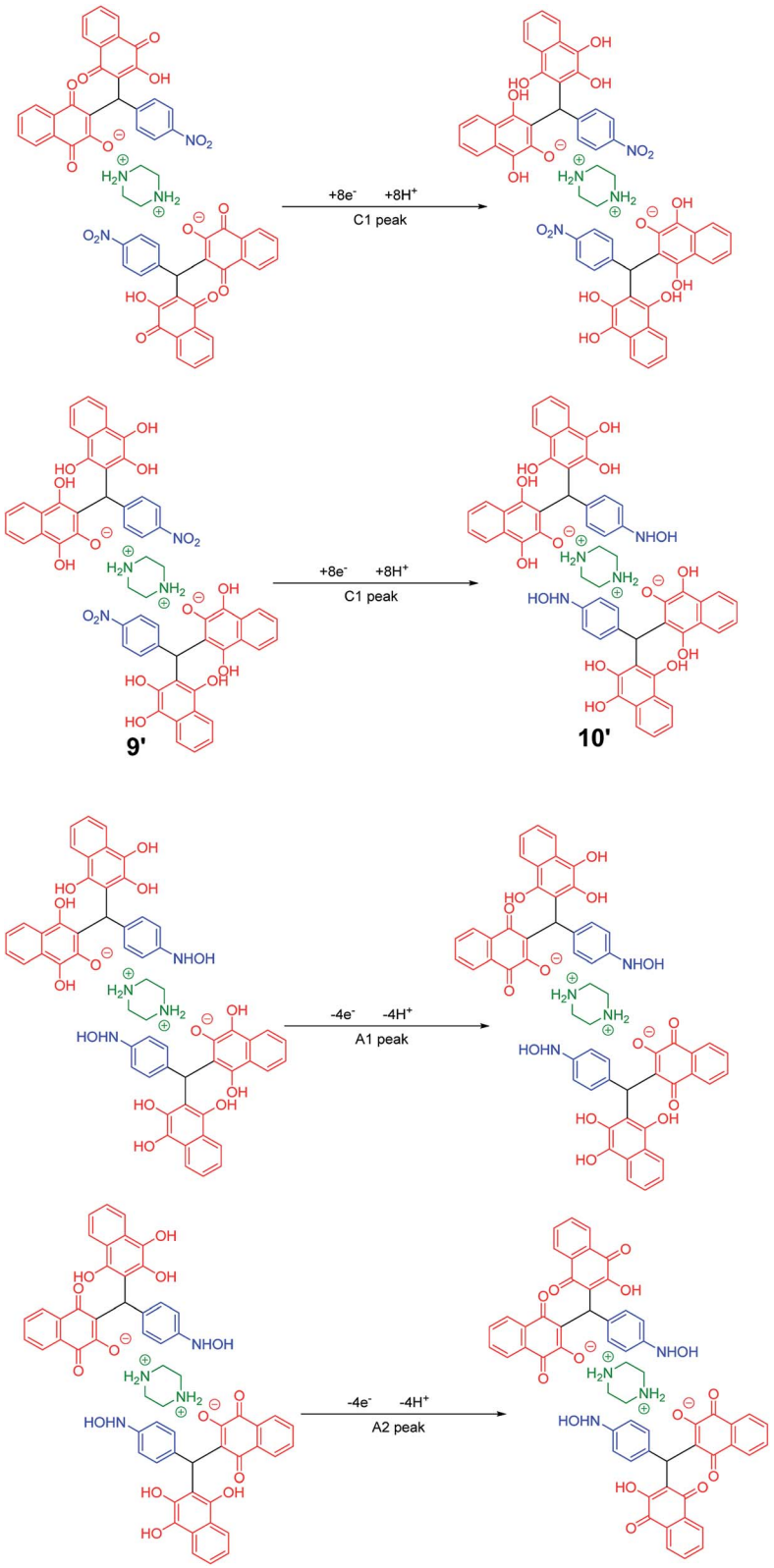

Scheme 5 Proposed mechanism of the electrochemical process in **6m** cyclic voltammogram in Fig. 1.

determined as model reaction to optimize the reaction conditions (Table 1).

2.5. Electrochemical test

Cyclic voltammograms of saturated solutions of **5b**, **6k**, **5c**, **6j**, **5a** and **6m** in DMSO are shown in Fig. 1. When the potential was scanned from −1.00 V to 0.00 V *vs.* Fc/Fc^{+}, the cyclic voltammograms do not show any oxidation or reduction, but upon scanning the electrode potential from −1.00 V to a more negative voltage (−2.00 V), the cyclic voltammogram exhibit one (C_1 for **5b**, **6k**, **5c**, **6j**, **5a**) or two (C_0 and C_1 for **5a** and **6m**) cathodic and two anodic peaks (A_1 and A_2). In the cyclic voltammograms of **5b** and **5c**, the C_1 peak is related to the reduction of **1** to **2** within a four-electron/four-proton process. The A_1 and A_2 peaks are related to the oxidation of **2** to **3** and **3** to **4** within a two-electron/two-proton process (Scheme 2).[48] In the cyclic voltammograms of **6k** and **6j**, the C_1 peak is related to the

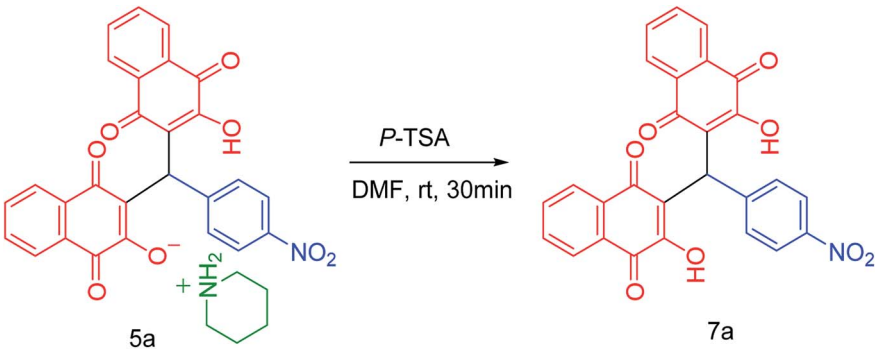

Scheme 6 Synthesis of **7a** *via* reaction of **5a**.

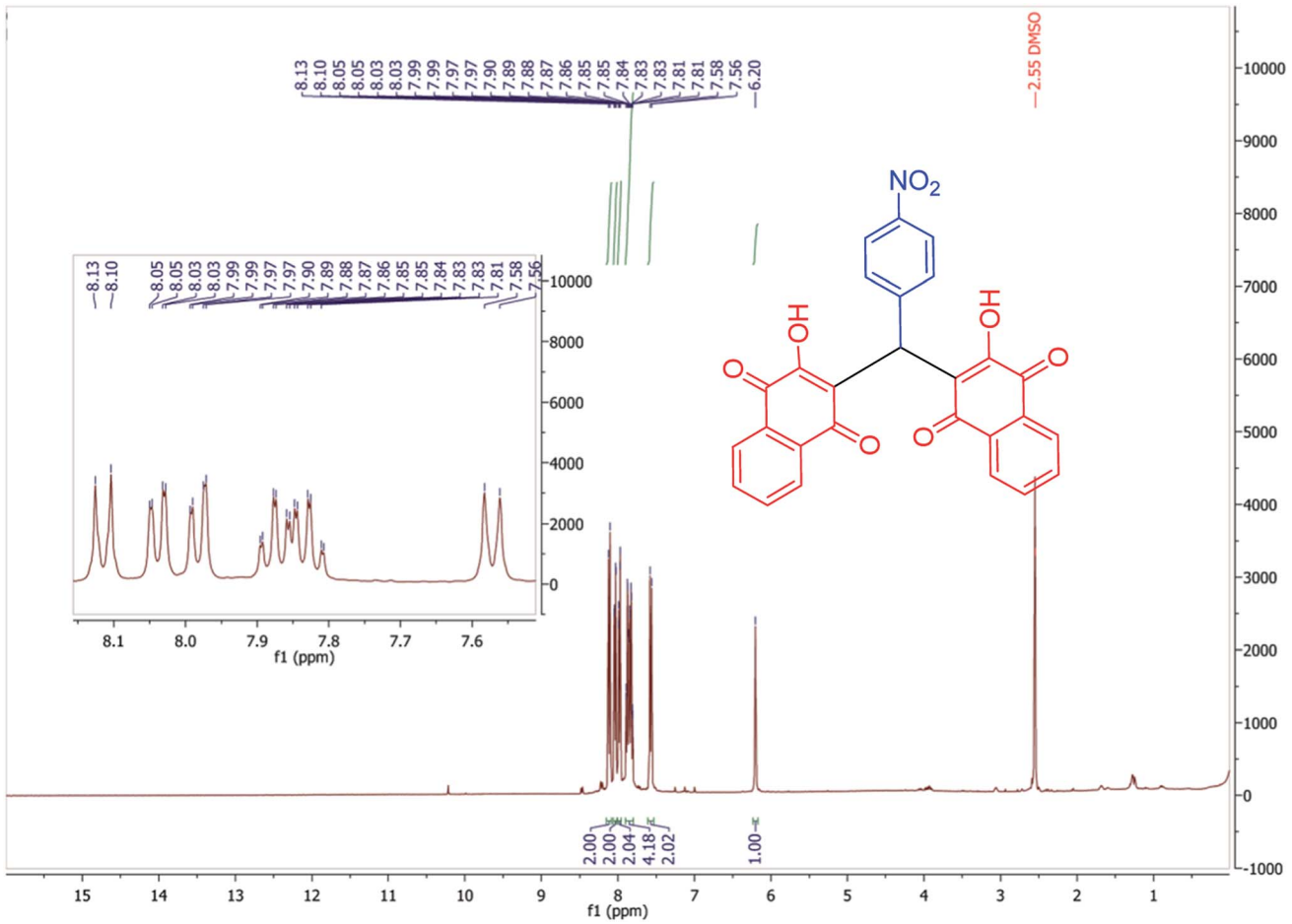

Fig. 2 ^{1}H NMR spectrum of product **7a**.

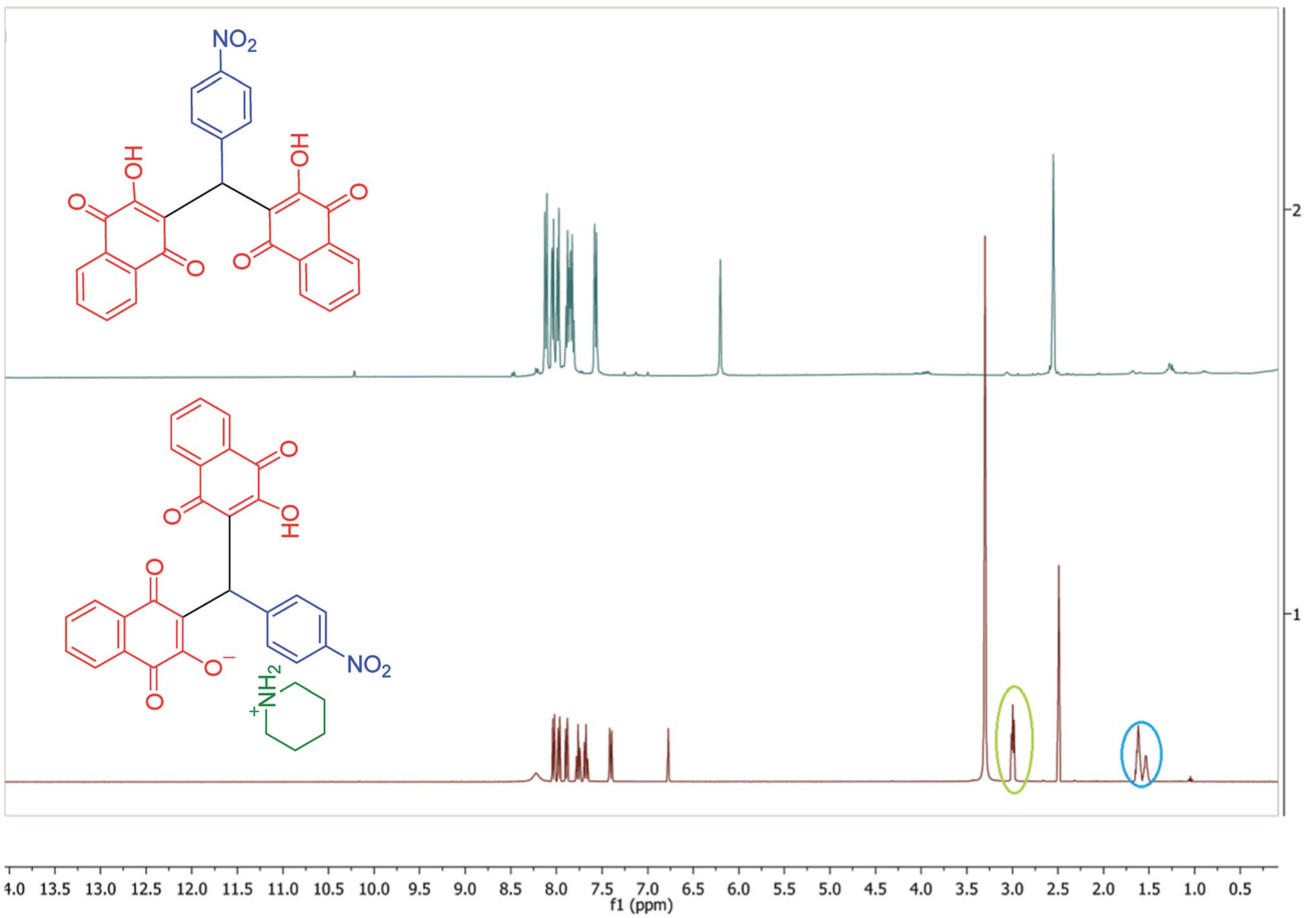

Fig. 3 Comparison of the ^{1}H NMR spectra of product **7a** and **5a**.

reduction of **5** to **6** within an eight-electron/eight-proton process, A_1 and A_2 peaks are related to the oxidation of **6** to **7** and **7** to **8** within a four-electron/four-proton process (Scheme 3).

In the cyclic voltammograms of **5a** and **6m**, a new irreversible cathodic peak (C_0) corresponding to the reduction of $-NO_2$ to –NHOH functional group (**9** and **9′** to **10** and **10′**), appears at a more negative potential (Fig. 1) (Schemes 4 and 5).[49]

3. Result and discussion

In continuation of our investigation, PCPs(Bi)N($CH_2PO_3H_2$)$_2$ was tested as nano heterogeneous catalyst for the synthesis of naphthoquinone derivatives based on piperazine and piperidine. As shown in Table 1, the best amount of catalyst was 10 mg PCPs(Bi)N($CH_2PO_3H_2$)$_2$ and reflux in water lead to the best yield (Table 1, entry 6). Different amounts of catalyst and different temperatures did not improve the yield or reaction time (Table 1 entries 1–10). To investigate the solvent effect on the reaction improvement, several solvents such as H_2O, DMF, EtOH, $CHCl_3$, EtOAc, CH_3CN, toluene (5 mL) and a solvent free reaction were tested and compared with reflux in water in the presence of 10 mg PCPs(Bi)N($CH_2PO_3H_2$)$_2$ (Table 1, entries 11–17). The results are summarized in Table 1.

To confirm of the structure product **5a**, the product was dissolved in ethanol in the present of *p*-TSA (1.0 eq.) which was stirred for 30 minutes (Scheme 6). After completing the reaction, the product was separated by filtration. By comparing the

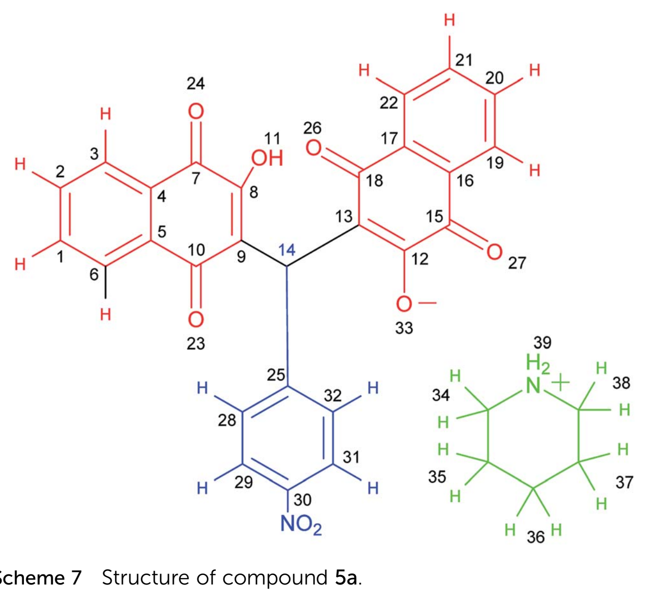

Scheme 7 Structure of compound **5a**.

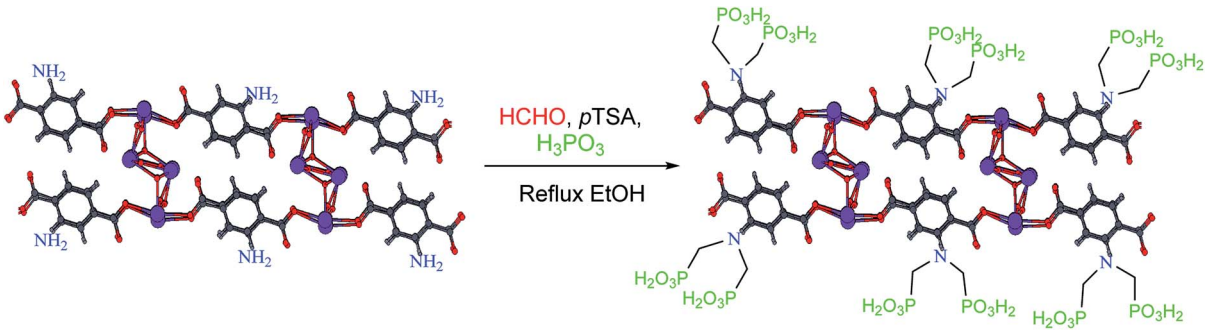

Scheme 8 Synthesis of PCPs(Bi)–BDC-NH_2 containing phosphorous acid functional groups.

initial product **5a** and the reaction product **7a** we confirmed the salt structure of **5a**. The structure of product **7a** was confirmed by ^{1}H NMR (Fig. 2 and 3) and by comparing its obtained physical data with those reported in the literature. We find, that the signals at 1.52–165 and 2.98–3.01 related to piperidinium cation is absent (Fig. 3).

3.1. Analytical data of compound 5a

After purification, the structures of the desired products (**5a–5j**) and (**6a–6n**) were fully characterized using various techniques such as FT-IR (Fig. S1†), ^{1}H NMR (Fig. S2†), ^{13}C NMR (DEPT-135) (Fig. S3†), ^{1}H^{1}H, COSY-NMR (Fig. S4–S6†), ^{1}H^{13}C, HSQC-NMR (Fig. S7 and S8†) and ^{1}H^{13}C, HMBC-NMR (Fig. S9–S12†). The structure of the compounds was presented in Scheme 7.

Orange solid; mp: 249–250 °C; IR (KBr): υ (cm^{-1}) = 3433, 3216 (NH_2), 3173 (C–H aromatic), 2929, 2854 (C–H aliphatic), 1676, 1638 (C=O), 1595, 1573, 1512, 1344 (NO_2). ^{1}H NMR (400 MHz, DMSO-d_6) δ 8.22 (s, 2H), 8.03 (d, J = 8.8 Hz, 2H), 7.97 (d, J = 7.6 Hz, 2H), 7.89 (d, J = 7.4 Hz, 2H), 7.76 (t, J = 7.4 Hz, 2H), 7.68 (t, J = 7.4 Hz, 2H), 7.41 (d, J = 8.6 Hz, 2H), 6.77 (s, 1H), 3.02–2.97 (m, 4H), 1.62 (p, J = 5.7 Hz, 4H), 1.54 (q, J = 5.3 Hz, 2H). ^{13}C NMR (DEPT-135) (100 MHz, DMSO-d_6) δ 183.4, 182.2, 164.7, 150.8, 145.2, 133.9, 133.2, 132.0, 131.0, 128.1, 125.8, 125.3, 123.1, 121.6, 43.8, 33.7, 22.2, 21.6. ^{1}H^{1}H COSY-NMR ((400, 400) MHz, DMSO-d_6) δ (8.04–8.02), (8.04–7.41), (8.02–7.41), (8.02–8.03), (7.98–7.97), (7.98–7.76), (7.96–7.76), (7.96–7.97), (7.90–7.90), (7.90–7.69), (7.88–7.69), (7.88–7.89), (7.78–7.77), (7.78–7.68), (7.78–7.98), (7.76–7.77), (7.74–7.98), (7.74–7.69), (7.74–7.77), (7.70–7.69), (7.70–7.76), (7.70–7.90), (7.68–7.69), (7.66–7.77), (7.66–7.90), (7.42–7.42), (7.42–8.04), (7.40–8.04), (7.39–7.40), (6.77–6.78), (3.30–3.31), (3.00–2.99), (2.98–1.63), (2.49–2.50), (1.61–1.54), (1.61–3.00), (1.60–1.62), (1.53–1.53), (1.51–1.63). ^{1}H^{13}C HSQC-NMR ((400, 100) MHz, DMSO-d_6) δ (8.03–123.03), (7.97–125.81), (7.89–125.26), (7.76–133.92), (7.68–132.07), (7.41–128.15), (6.77–33.81), (2.99–43.87), (2.49–39.86), (1.62–22.28), (1.53–21.77). ^{1}H^{13}C, HMBC-NMR ((400, 100) MHz, DMSO-d_6) δ (8.24–123.25), (8.11–125.68), (8.03–145.41), (8.03–151.00), (8.03–123.20), (7.97–131.61), (7.97–182.45), (7.90–134.43), (7.90–183.50), (7.76–133.36), (7.71–125.88), (7.70–125.73), (7.68–131.23), (7.41–128.33), (7.41–33.87), (7.41–145.40), (6.78–128.40), (6.78–182.43), (6.78–164.88), (6.78–151.01), (6.78–121.80), (3.00–44.04), (3.00–21.46), (3.00–23.01), (2.50–39.90), (1.63–44.12), (1.61–21.58), (1.54–22.43), (1.52–43.90).

4. Synthesis of porous coordination polymer (PCPs) (Bi)–BDC-NH_2

In a Teflon-lined bomb, a mixture of $Bi(NO_3)\cdot 5H_2O$ (1.0 mmol, 0.485 g) and 2-aminoterephthalic acid (2.0 mmol, 0.332 g) was putted in the oven at 180 °C for 5 days. Then the mixture was slowly cooled to room temperature. Then the porous coordination polymer containing bismuth formed a creamy precipitate which was washed with DMF to remove the unreacted ligand. The PCPs (Bi)–BDC-NH_2 was isolated by vacuum filtration.[13] Based on the data obtained from XRD, the structure and morphology of PCPs(Bi)–BDC-NH_2 is similar to what was observed for PCPs(Bi)–BDC-NO_2.[13] After verifying the structure, the polymer was applied for the synthesis of PCPs(Bi) $N(CH_2PO_3H_2)_2$. In a 50 mL round-bottomed flask PCPs(Bi)–BDC-NH_2 (1.0 g), paraformaldehyde (8.0 mmol, 0.54 g), phosphorous acid (8.0 mmol, 1.476 g), p-TSA (1.0 mmol, 0.172 g) and

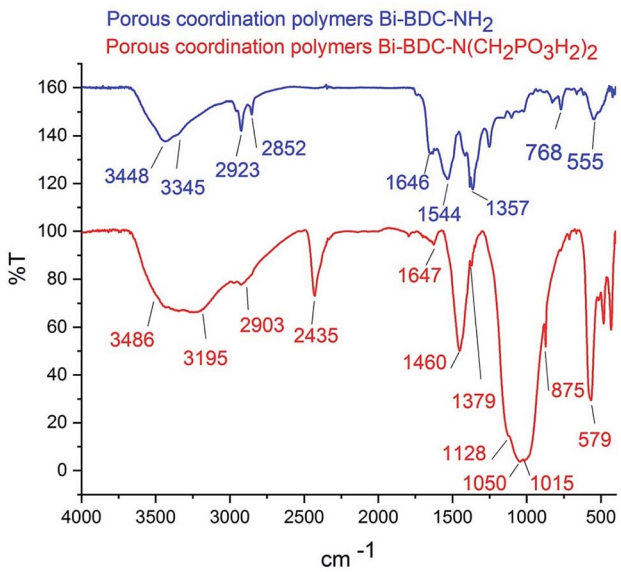

Fig. 4 FT-IR spectra of PCPs(Bi)BDC-NH_2 and PCPs(Bi)$N(CH_2PO_3H_2)_2$ in KBr.

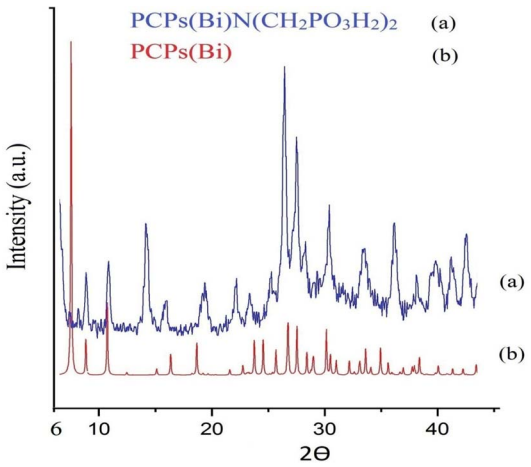

Fig. 5 Comparison XRD patterns of the PCPs(Bi) and PCPs(Bi) $N(CH_2PO_3H_2)$.

ethanol (15 mL) were mixed and refluxed for 18 hours. After this time, a yellow precipitate was isolated by centrifugation (1000 rpm, 10 min). The residue was dried under vacuum to obtain PCPs(Bi)$N(CH_2PO_3H_2)_2$ (1.65 g) (Scheme 8).

In continuation our investigations for developing of the knowledge of catalytic systems, catalytic systems and organic methodology, herein we wish to expand the porous catalysts. With this aim, we have prepared a novel functionalized porous coordination polymer (PCPs) linked to phosphorous acid groups in the presence *p*-TSA and paraformaldehyde under ethanol reflux (Scheme 8). PCPs(Bi)$N(CH_2PO_3H_2)_2$ was characterized by FT-IR and XRD spectroscopy, elemental mapping analysis (DEX), the scanning electron microscopy (SEM), N_2 adsorption–desorption isotherm (BET), thermal gravimetric (TG), derivative thermal gravimetric (DTG), differential thermal (DTA), transmission electron microcopy (TEM).

The FT-IR spectra of PCPs(Bi)BDC-NH_2 and PCPs(Bi) $N(CH_2PO_3H_2)_2$ were compared in Fig. 4. The broad peak 2600–3500 cm^{-1} is related to OH of PO_3H_2 functional groups. The aromatic C–H and C=C stretches bands are respectively at 2923 and 1647 cm^{-1}. The absorption bands at 1015 and 1050 cm^{-1} are related to P–O bond stretching and the band at 1128 cm^{-1} is related to P=O.[50] Furthermore, peaks of Bi–O of octahedral BiO_6 appeared at 875 and 579 cm^{-1} respectively[51] (Fig. 4). The FT-IR spectrum difference between PCPs(Bi)BDC-NH_2 and PCPs(Bi)$N(CH_2PO_3H_2)_2$ verified the structure of the catalyst.

The morphology and structure of the of PCPs(Bi) $N(CH_2PO_3H_2)$ was studied using XRD (Fig. 5). PCPs(Bi)[13] and PCPs(Bi)$N(CH_2PO_3H_2)$ were compared in the range of 6–44° using XRD as shown in Fig. 5. The peaks of Bi–O of PCPs(Bi) in $2\theta = 8.8, 10.76, 18.6, 26.8$ and 27.6 and PO_3H_2 in $2\theta = 23.4, 30.2, 33.7$ and 36.2 are observed in the XRD pattern, which is consistent with previously paper.[52,53] The SEM images of the PCPs(Bi)$N(CH_2PO_3H_2)_2$ catalyst reveal that the particles shape resembles cauliflowers and the particle size is within the range of the 38–49 nm (Fig. 6).

The present elements of PCPs(Bi)$N(CH_2PO_3H_2)_2$ can be seen using energy-dispersive X-ray spectroscopy (EDX) and elemental mapping analysis and in the energy-dispersive X-ray spectroscopy (EDX) mode in scanning electron microscopy (SEM). In EDX elemental mapping analysis, bismuth (61.82%), carbon (8.56%), nitrogen (2.62%), oxygen (17.24%) and phosphor (9.77%) were confirmed in the structure of PCPs(Bi) $N(CH_2PO_3H_2)_2$ (Fig. 7).

Transmission Electron Microcopy (TEM) images of PCPs(Bi) $N(CH_2PO_3H_2)_2$ are presented in Fig. 8. In agreement with SEM a cross-linked nanostructure of PCPs-catalyst was confirmed. The particles of PCPs(Bi)$N(CH_2PO_3H_2)_2$ are approximately 30–50 nm with a narrow size distribution.

Nitrogen adsorption–desorption isotherm after Brunauer Emmett and Teller (BET) of PCPs(Bi)$N(CH_2PO_3H_2)_2$ was also studied in Fig. S13.† Mean pore diameter, BET surface area, and

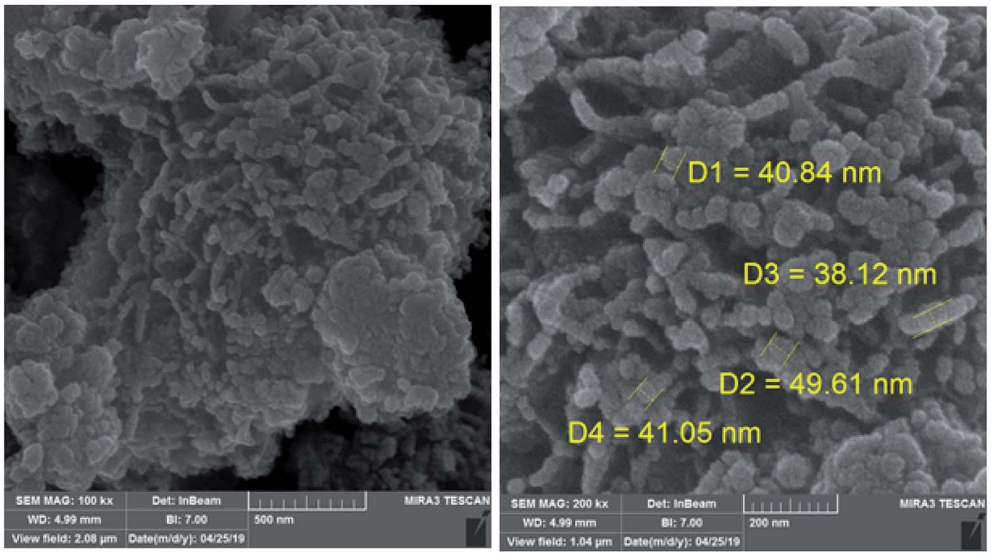

Fig. 6 SEM of PCPs(Bi)$N(CH_2PO_3H_2)_2$.

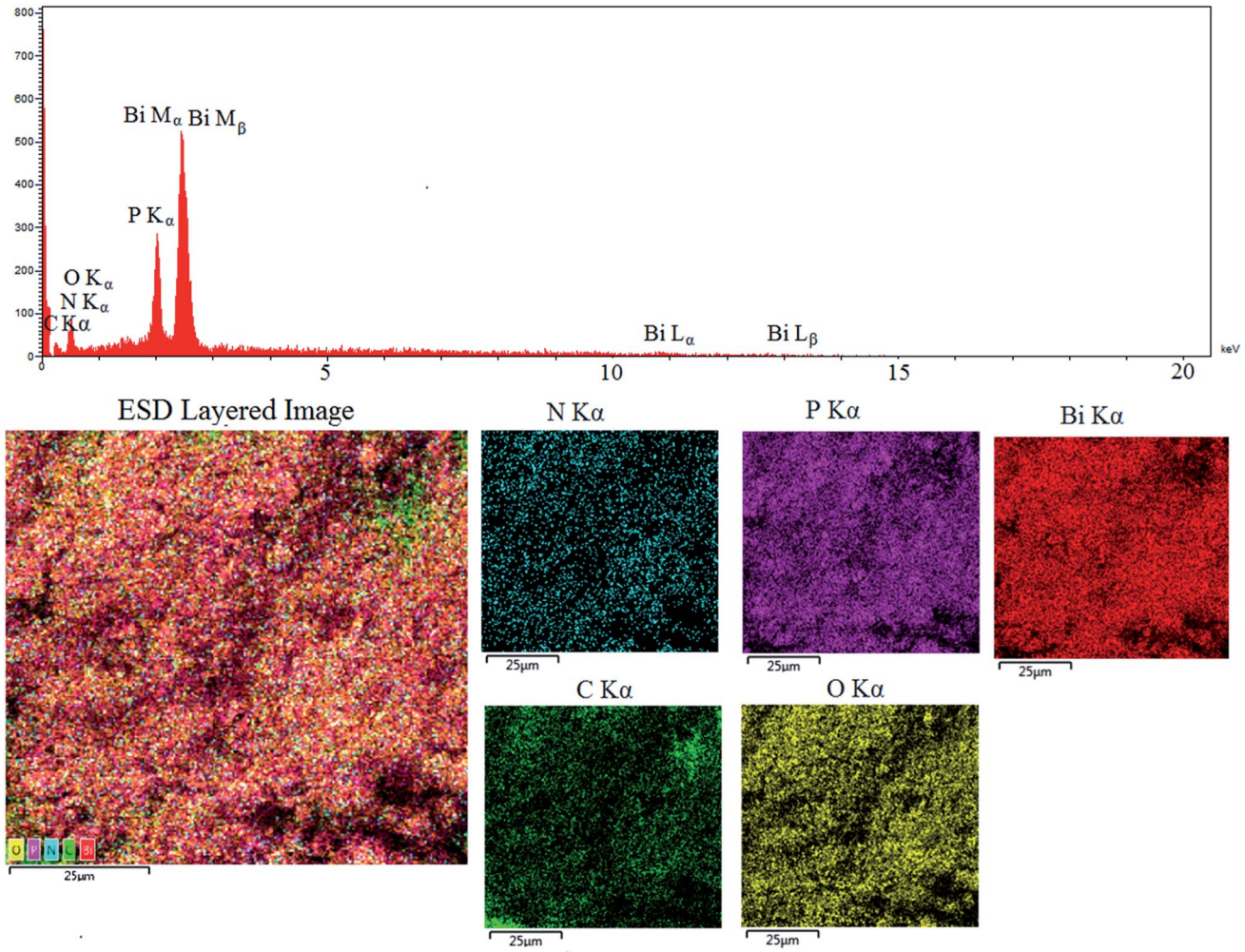

Fig. 7 Energy-dispersive X-ray spectroscopy (EDX), elemental mapping analysis of PCPs(Bi)N$(CH_2PO_3H_2)_2$.

total pore volume of PCPs(Bi)N$(CH_2PO_3H_2)_2$ are 38.8 nm, 22 m^2 g^{-1} and 0.2 cm^3 g^{-1}.

Thermal Gravimetric (TG) and derivative thermal gravimetric (DTG) analysis of PCPs(Bi)N$(CH_2PO_3H_2)_2$ are shown in the Fig. 9. Two decline stages were observed for PCPs(Bi) N$(CH_2PO_3H_2)_2$ in the Fig. 9. The weight loss was related to evaporation of solvent (organic and water). Based on previously work, the weight loss of the first step in TG patterns is related to the exit of solvents used in the course of synthesis of described catalyst.[54–56] The results show that the catalyst can be used up to 228 °C. At this temperature to the polymer exhausts PO_3H_2 groups and the structure of PCPs(Bi)N$(CH_2PO_3H_2)_2$ is decomposed (Fig. 9).

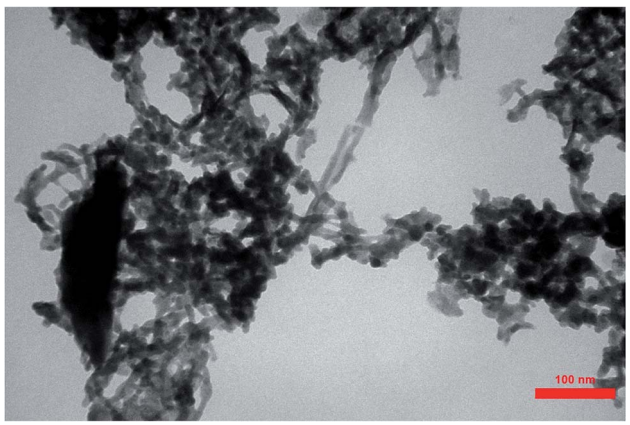

Fig. 8 TEM of PCPs(Bi)N$(CH_2PO_3H_2)_2$.

5. Catalytic properties of (PCPs) (Bi)–BDC-NH_2

5.1. Synthesis of mono and bis naphthoquinone based on salts of piperidine

In a 25 mL round-bottomed flask, a mixture of 2-hydroxynaphthalene-1,4-dione (2.0 mmol, 0.348 g), piperidine (1.0 mmol, 0.085 g), aryl aldehyde (1.0 mmol) and PCPs(Bi) N$(CH_2PO_3H_2)_2$ (10 mg) as catalyst were stirred in an aqueous solution under reflux condition. After completion of the reaction which was detected by thin layer chromatography (TLC) (*n*-hexane/EtOAc; 1 : 2), the reaction mixture was cooled to room

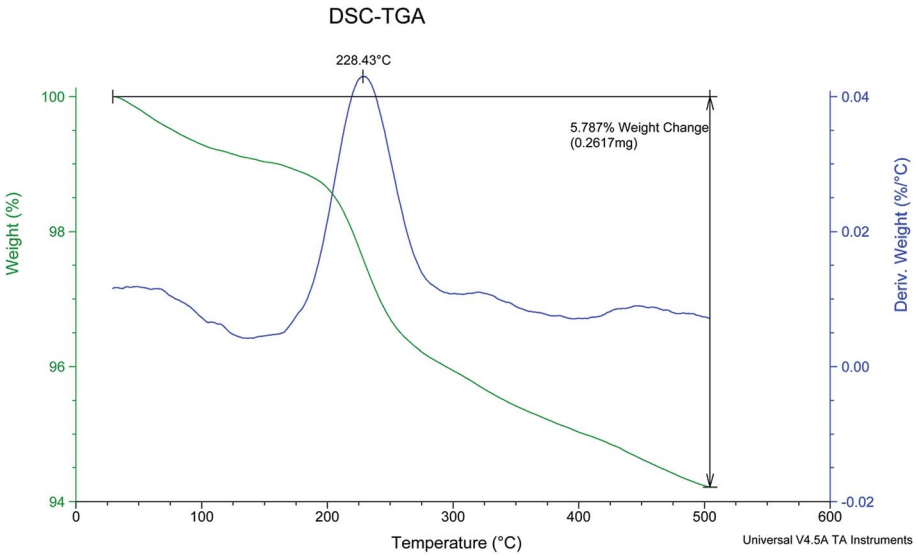

Fig. 9 TG and DTG analysis of PCPs(Bi)N$(CH_2PO_3H_2)_2$.

Table 2 Evaluation of various catalyst for the synthesis of **5b** in comparison with PCPs(Bi)N$(CH_2PO_3H_2)_2$ under water reflux

Entry	Catalyst	(mol% or mg)	Time (h)	Yield (%)	TON	TOF
1	[Py-SO_3H]Cl[57]	10	1.5	62	620	413.3
2	NH_4NO_3	10	5	—	—	—
3	CF_3SO_3H	10	5	Trace	—	—
4	$Al(HSO_4)_3$	10	5	37	370	74
5	$H_3[p(W_3O_{10})_4]\cdot XH_2O$	10	4	30	300	75
6	$Mg(NO_3)_2\cdot 6H_2O$	10	4	—	—	
7	GTBSA[58]	10	2	68	680	340
8	*p*-TSA	10	5	Trace	—	—
9	Trichloroisocyanuric acid	10	5	32	320	64
10	H_3PO_3	10	1.5	73	730	486
11	[Fe_3O_4@SiO_2@Pr-DABCO-SO_3H]Cl_2 (ref. 59)	10	2	72	—	—
12	APVPB[60]	10 mg	4	58	—	—
13	Fe_3O_4	10 mg	5	—	—	—
14	SBISAC[61]	10 mg	2	55	—	—
15	SSA[62]	10 mg	1.5	45	—	—
16	[PVI-SO_3H]Cl[63]	10 mg	1	56	—	—
17	PCPs(Bi)BDC-NH_2	10 mg	4	24	—	—
18	**PCPs(Bi)N$(CH_2PO_3H_2)_2$**	**10 mg**	**5 (min)**	**95**	—	—

temperature. Then, warm acetone (10 mL) was added to the mixture for separation of the catalyst by centrifugation (1000 rpm, 10 min). Then, the obtained product was washed with water/ethanol (1 : 1) Scheme 1.

5.2. Synthesis of mono and bis naphthoquinone based on salts of piperazine

In a 25 mL round-bottomed flask, a mixture of 2-hydroxynaphthalene-1,4-dione (4.0 mmol, 0.696 g), piperazine (1.0 mmol, 0.086 g), aryl aldehyde (2.0 mmol) and PCPs(Bi)N$(CH_2PO_3H_2)_2$ (10 mg) as catalyst were stirred in an aqueous solution under reflux condition. After completion of the reaction which was detected by thin layer chromatography (TLC) (*n*-hexane/EtOAc; 1 : 2), the reaction mixture was cooled to room

temperature. Then, warm acetone (10 mL) was added to the mixture for separation of the catalyst by centrifugation (1000 rpm, 10 min). Then, the obtained product was washed with water/ethanol (1 : 1) Scheme 1.

5.3. Catalytic potential of PCPs(Bi)N$(CH_2PO_3H_2)_2$

We further investigated the efficiency of PCPs(Bi)N$(CH_2PO_3H_2)_2$ for the synthesis of **5b** for the reaction of 2-hydroxynaphthalene-1,4-dione (2.0 mmol, 0.348 g), piperidine (1.0 mmol, 0.085 g) and benzaldehyde (1.0 mmol, 0.106 g) under the above mentioned optimized reaction conditions. Various organic and inorganic acid catalysts for the above reaction were also tested for comparison (Table 2). As Table 2 indicates, PCPs(Bi)N$(CH_2PO_3H_2)_2$ is the best catalyst for the synthesis of

Table 3 Synthesis of piperidin-1-ium 3-((3-hydroxy-1,4-dioxo-1,4-dihydronaphthalen-2-yl)(phenyl)methyl)-1,4-dioxo-1,4-dihydronaphthalen-2-olate (**5a–5j**) and piperazine-1,4-diium 3-((1,4-dioxo-1,4-dihydronaphthalen-2-yl)(phenyl)methyl)-1,4-dioxo-1,4-dihydronaphthalen-2-olate derivatives in the presence of PCPs(Bi)N($CH_2PO_3H_2$)$_2$

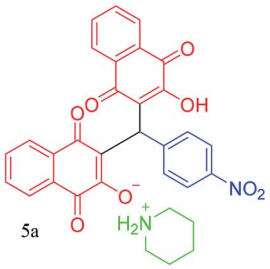

mp ºC: 249-250, Yield (%): 95
Time: 4 (min)

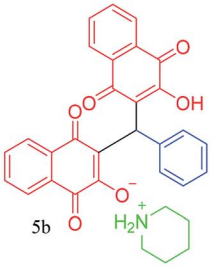

mp ºC: 184-185, Yield (%): 92
Time: 5 (min)

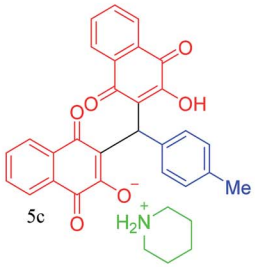

mp ºC: 239-240,Yield (%): 88
Time: 8 (min)

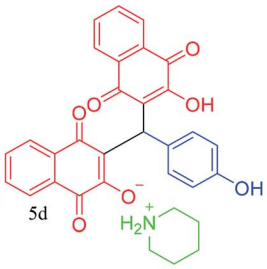

mp ºC: 230-232, Yield (%): 87
Time: 10 (min)

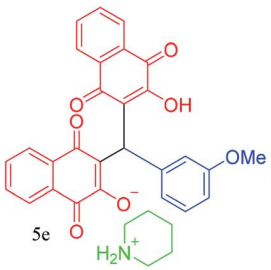

mp ºC: 215, Yield (%): 85
Time: 9(min)

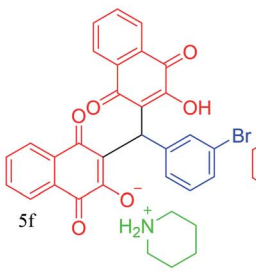

mp ºC: 248-250, Yield (%): 84
Time: 15 (min)

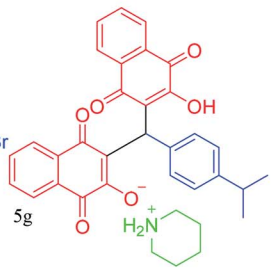

mp ºC: 240-242, Yield (%): 89
Time: 8 (min)

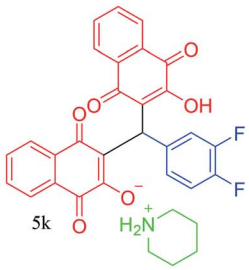

mp ºC: 260-263, Yield (%): 86
Time: 7 (min)

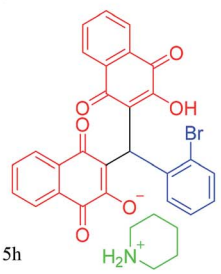

mp ºC: 216-218, Yield (%): 83
Time: 15(min)

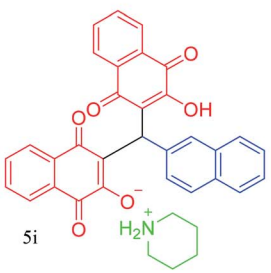

mp ºC: 259-260, Yield (%): 88
Time: 12 (min)

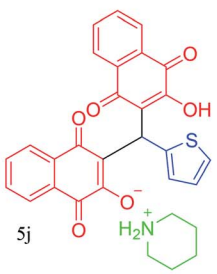

mp ºC: 240-241Yield (%): 86
Time: 10 (min)

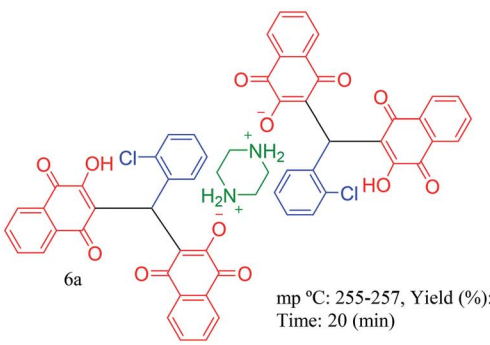

mp ºC: 255-257, Yield (%): 89
Time: 20 (min)

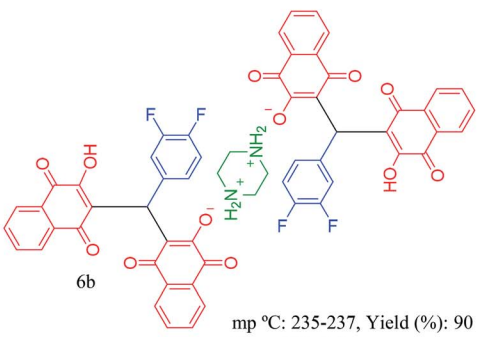

mp ºC: 235-237, Yield (%): 90
Time: 15(min)

Table 3 (contd.)

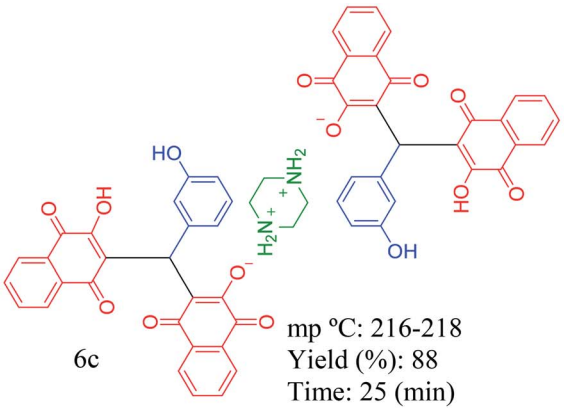

6c

mp °C: 216-218
Yield (%): 88
Time: 25 (min)

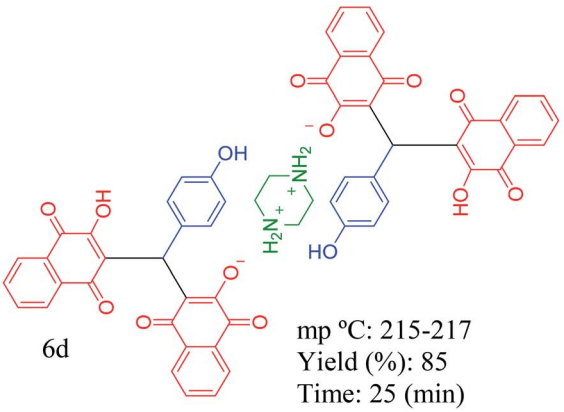

6d

mp °C: 215-217
Yield (%): 85
Time: 25 (min)

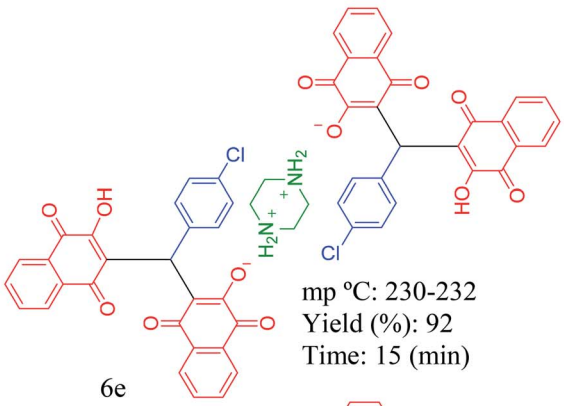

6e

mp °C: 230-232
Yield (%): 92
Time: 15 (min)

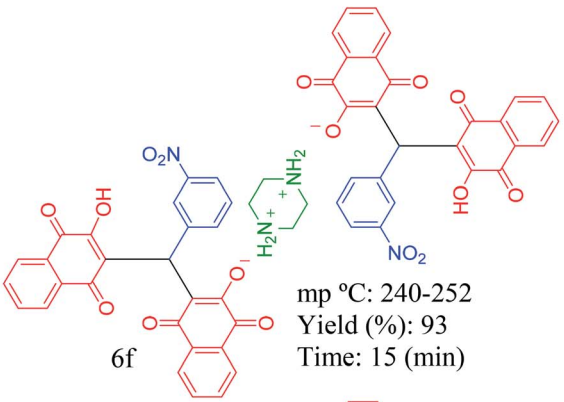

6f

mp °C: 240-252
Yield (%): 93
Time: 15 (min)

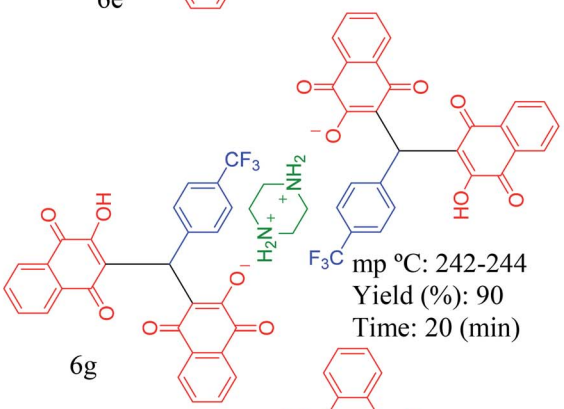

6g

mp °C: 242-244
Yield (%): 90
Time: 20 (min)

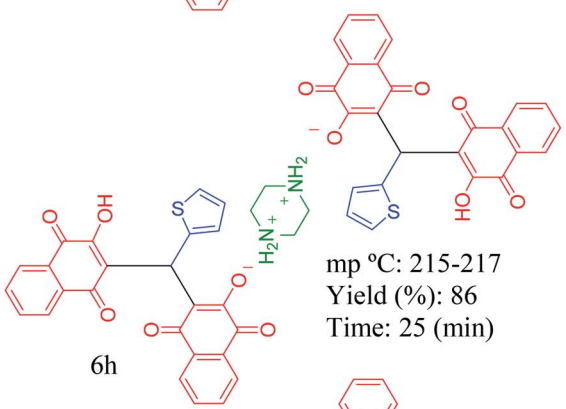

6h

mp °C: 215-217
Yield (%): 86
Time: 25 (min)

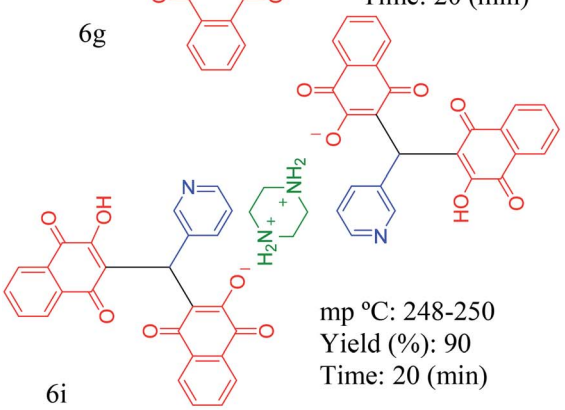

6i

mp °C: 248-250
Yield (%): 90
Time: 20 (min)

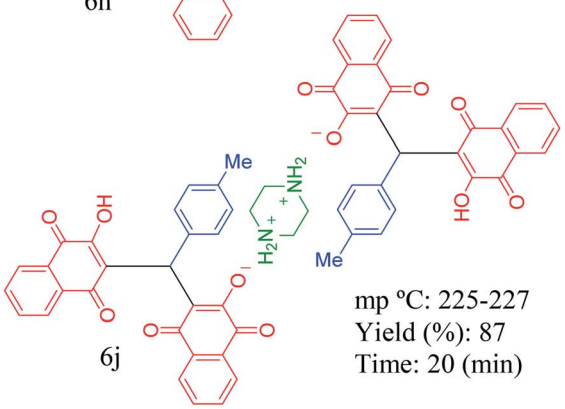

6j

mp °C: 225-227
Yield (%): 87
Time: 20 (min)

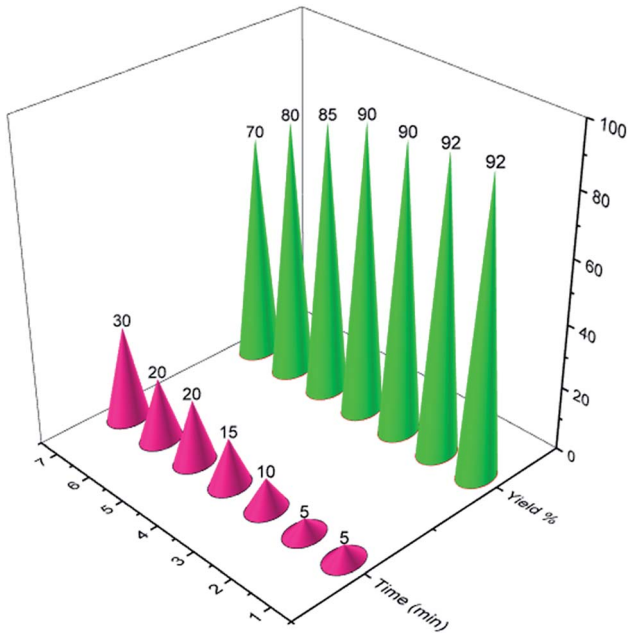

Fig. 10 Recyclability of PCPs(Bi)N$(CH_2PO_3H_2)_2$ for the synthesis naphthoquinone derivatives.

naphthoquinone derivatives as salts of piperazine or piperidine, due to the shorter reaction times, higher yields and amount of applied catalyst.

Then, PCPs(Bi)N$(CH_2PO_3H_2)_2$ was tested as heterogeneous catalyst. The efficiency and applicability were studied for the reaction of hydroxynaphthalene-1,4-dione (4 mmol or 2 mmol), piperazine or piperidine (1.0 mmol), aryl aldehyde (2.0 mmol or 1.0 mmol). As shown in Table 2, this method is suitable for the synthesis of naphthoquinone derivatives based on piperazine and piperidine (**5a–5j**) and (**6a–6n**) (Table 3) in high to excellent yields (82–95%) with in relatively short reaction times (4–30 min). As shown in Table 3, all aldehydes including benzaldehyde as well as other aromatic aldehydes possessing electron-releasing substituents, electron withdrawing substituents, basic groups or halogens afforded the desired naphthoquinone compounds as salts of piperazine or piperidine.

Finally, for checking the reusability of the described catalyst for the synthesis of naphthoquinone derivatives, PCPs(Bi)N$(CH_2PO_3H_2)_2$ was examined in a model reaction. We used 2-hydroxynaphthalene-1,4-dione (2.0 mmol, 0.348 g), piperidine (1.0 mmol, 0.085 g) and benzaldehyde (1.0 mmol, 0.106 g). The results show that the catalyst has the potential to be reused up to 6 times without significant yield reduction (Fig. 10).

6. Conclusion

In summary, a porous coordinated polymer (PCPs) was designed, synthesized and applied as a novel, efficient and functionalized phosphorus acid PCPs(Bi)N$(CH_2PO_3H_2)_2$ catalyst. PCPs(Bi)N$(CH_2PO_3H_2)_2$ was prepared using a reaction of PCPs(Bi)BDC-NH_2, paraformaldehyde and phosphorus acid (H_3PO_3). The described coordinated polymer PCPs(Bi)N$(CH_2PO_3H_2)_2$ was also tested as a porous catalyst for the synthesis of new mono and bis-naphthoquinone-based salts were characterized with ^{1}H, ^{13}C NMR, ^{13}C NMR (DEPT-135), ^{1}H^{1}H Cosy, ^{1}H^{13}C HSQC, ^{1}H^{13}C HMBC, FT-IR and HR-Mass. Since that henna-based salts compounds are good candidates for electrochemical investigation, the electrochemical action of the obtained products was also investigated and presented. The present work can open up a new perspective in the course of rational design, synthesis and applications of task-specific biological based hennotannic acid (2-hydroxynaphthalene-1,4-dione or henna) based molecules. Some of the major advantages of this work are high yield of products, short reaction times, facile workup and reusability of the presented catalyst.

Conflicts of interest

There are no conflicts to declare.

Acknowledgements

We thank the Bu-Ali Sina University, IMC University of Applied Sciences, Groningen University, National Elites Foundation and Iran National Science Foundation (INSF) (grant number: 98020070) for financial support.

References

1 S. Rojas-Buzo, P. García-García and A. Corma, *Green Chem.*, 2018, **20**, 3081–3091.
2 U. Gulati, U. C. Rajesh, D. S. Rawat and J. M. Zaleski, *Green Chem.*, 2020, **22**, 3170–3177.
3 S. Rostamnia and M. Jafari, *Appl. Organomet. Chem.*, 2017, **31**, 3584.
4 T. Friščić, in *Ball Milling Towards Green Synthesis: Applications, Projects, Challenges*, The Royal Society of Chemistry, 2015, pp. 151–189.
5 H. Alamgholiloo, S. Rostamnia, A. Hassankhani and R. Banaei, *Synlett*, 2018, **29**, 1593–1596.
6 S. Rostamnia and F. Mohsenzad, *Mol. Catal.*, 2018, **445**, 12–20.
7 J. Liang, Y.-B. Huang and R. Cao, *Coord. Chem. Rev.*, 2019, **378**, 32–65.
8 S. Rostamnia and H. Alamgholiloo, *Catal. Lett.*, 2018, **148**, 2918–2928.
9 S. Rostamnia, H. Alamgholiloo and M. Jafari, *Appl. Organomet. Chem.*, 2018, **32**, 4370.
10 S. Rostamnia and Z. Karimi, *Inorg. Chim. Acta*, 2015, **428**, 133–137.
11 A. Thirumurugan, W. Li and A. K. Cheetham, *Dalton Trans.*, 2012, **41**, 4126–4134.
12 Y.-Q. Sun, S.-Z. Ge, Q. Liu, J.-C. Zhong and Y.-P. Chen, *CrystEngComm*, 2013, **15**, 10188–10192.
13 A. C. Wibowo, M. D. Smith and H.-C. zur Loye, *CrystEngComm*, 2011, **13**, 426–429.
14 S. Iram, M. Imran, F. Kanwal, Z. Iqbal, F. Deeba and Q. J. Iqbal, *Z. Anorg. Allg. Chem.*, 2019, **645**, 50–56.

15 M. Matsubara, A. Suzumura, S. Tajima and R. Asahi, *ACS Comb. Sci.*, 2019, **21**, 400–407.
16 R. Hobbs, D. Thorek, D. Abou, A. Josefsson, W. Bolch and G. Sgouros, *J. Med. Imaging Radiat. Oncol.*, 2019, **50**, 34–35.
17 T. Lu, Z. Du, J. Liu, H. Ma and J. Xu, *Green Chem.*, 2013, **15**, 2215–2221.
18 S. Hasegawa, S. Horike, R. Matsuda, S. Furukawa, K. Mochizuki, Y. Kinoshita and S. Kitagawa, *J. Am. Chem. Soc.*, 2007, **129**, 2607–2614.
19 S. Shimomura, S. Horike and S. Kitagawa, in *Stud. Surf. Sci. Catal.*, Elsevier, 2007, vol. 170, pp. 1983–1990.
20 J. B. Marcus, in *Culinary Nutrition*, ed. J. B. Marcus, Academic Press, San Diego, 2013, pp. 279–331.
21 R. Heaney, *Vitamin D*, Academic Press, San Diego, 3rd edn, 2011.
22 P. J. Withers, R. Sylvester-Bradley, D. L. Jones, J. R. Healey and P. J. Talboys, *Rethinking phosphorus management in the food chain*, ACS Publications, 2014, pp. 6523–6530.
23 B. Aleksandra, B. Karolina, K.-S. Jolanta and D. Jolanta, *Open access peer-reviewed chapter*, 2019, DOI: 10.5772/intechopen.85723.
24 Y. Liu and J. Chen, in *Encyclopedia of Ecology*, ed. B. Fath, Elsevier, Oxford, 2nd edn, 2014, pp. 181–191.
25 D. Zhao and R. Wang, *Chem. Soc. Rev.*, 2012, **41**, 2095–2108.
26 H. Sepehrmansouri, M. Zarei, M. A. Zolfigol, A. R. Moosavi-Zare, S. Rostamnia and S. Moradi, *Mol. Catal.*, 2020, **481**, 110303.
27 B. List and D. Díaz-Oviedo, *Synfacts*, 2019, **15**, 0303.
28 L. Zhang, S.-H. Xiang, J. Wang, J. Xiao, J.-Q. Wang and B. Tan, *Nat. Commun.*, 2019, **10**, 566.
29 P. Babula, V. Adam, L. Havel and R. Kizek, *Ceska Slov. Farm.*, 2007, **56**, 114–120.
30 A. G. F. Shoair, *J. Coord. Chem.*, 2012, **65**, 3511–3518.
31 M. Zarei, M. A. Zolfigol, A. R. Moosavi-Zare and E. Noroozizadeh, *J. Iran. Chem. Soc.*, 2017, **14**, 2187–2198.
32 M. A. Zolfigol, A. Khazaei, S. Alaie and S. Baghery, *Can. J. Chem.*, 2017, **95**, 560–570.
33 A. Bazgir, Z. N. Tisseh and P. Mirzaei, *Tetrahedron Lett.*, 2008, **49**, 5165–5168.
34 A. Rahmati, *Chin. Chem. Lett.*, 2010, **21**, 761–764.
35 D. M. Rekik, S. B. Khedir, A. Daoud, K. K. Moalla, T. Rebai and Z. Sahnoun, *Skin Pharmacol. Physiol.*, 2019, 1–12, DOI: 10.1159/000501730.
36 B. R. Mikhaeil, F. A. Badria, G. T. Maatooq and M. M. Amer, *Z. Naturforsch., C: J. Biosci.*, 2004, **59**, 468–476.
37 S. Bonjar, *J. Ethnopharmacol.*, 2004, **94**, 301–305.
38 M. Natarajan and D. Lalithakumari, *Curr. Sci.*, 1987, **56**, 1021–1022.
39 S. Satish, D. Mohana, M. Ranhavendra and K. Raveesha, *J. Agric. Sci. Technol.*, 2007, **3**, 109–119.
40 S. Gupta, M. Ali, K. Pillai and M. Sarwar Alam, *Fitoterapia*, 1993, **64**, 365.
41 M. Ali and M. Grever, *Fitoterapia*, 1998, **69**, 181–183.
42 N. Sultana, M. I. Choudhary and A. Khan, *J. Enzyme Inhib. Med. Chem.*, 2009, **24**, 257–261.
43 T. Okpekon, S. Yolou, C. Gleye, F. Roblot, P. Loiseau, C. Bories, P. Grellier, F. Frappier, A. Laurens and R. Hocquemiller, *J. Ethnopharmacol.*, 2004, **90**, 91–97.
44 M. M. Khoram, D. Nematollahi, S. Momeni, M. Zarei and M. A. Zolfigol, *Electrochim. Acta*, 2019, **326**, 134990.
45 G. Abbas, Z. Hassan, A. Al-Harrasi, A. khan, A. Al-Adawi and M. Ali, *J. Mol. Struct.*, 2019, **1195**, 462–469.
46 P. Ravichandiran, S. A. Subramaniyan, S. Y. Kim, J. S. Kim, B. H. Park, K. S. Shim and D. J. Yoo, *ChemMedChem*, 2019, **14**, 532–544.
47 S. Khazalpour and D. Nematollahi, *J. Electrochem. Soc.*, 2016, **163**, 133–137.
48 H. Yin, Q. Zhang, Y. Zhou, Q. Ma, L. Zhu and S. Ai, *Electrochim. Acta*, 2011, **56**, 2748–2753.
49 B. Mokhtari, D. Nematollahi and H. Salehzadeh, *Green Chem.*, 2018, **20**, 1499–1505.
50 V. Jagodić, *Croat. Chem. Acta*, 1977, **49**, 127–133.
51 H.-R. Bahari, H. A. Sidek, F. R. M. Adikan, W. M. Yunus and M. K. Halimah, *Int. J. Mol. Sci.*, 2012, **13**, 8609–8614.
52 N. Motakef-Kazemi and M. Yaqoubi, *Iran. J. Pharm. Res.*, 2020, 1217–1223.
53 Y. Chen, Y. Zhou, Q. Yao, Y. Bu, H. Wang, W. Wu and W. Sun, *J. Appl. Polym. Sci.*, 2015, 132.
54 T. Qu, Q. Wei, C. Ordonez, J. Lindline, M. Petronis, M. S. Fonari and T. Timofeeva, *Crystals*, 2018, **8**, 162.
55 K. Vikrant, Y. Qu, J. E. Szulejko, V. Kumar, K. Vellingiri, D. W. Boukhvalov, T. Kim and K.-H. Kim, *Nanoscale*, 2020, **12**, 8330–8343.
56 B. Ghalei, K. Sakurai, Y. Kinoshita, K. Wakimoto, A. P. Isfahani, Q. Song, K. Doitomi, S. Furukawa, H. Hirao and H. Kusuda, *Nat. Energy*, 2017, **2**, 17086.
57 A. R. Moosavi-Zare, M. A. Zolfigol, M. Zarei, A. Zare, V. Khakyzadeh and A. Hasaninejad, *Appl. Catal., A*, 2013, **467**, 61–68.
58 M. Zarei, H. Sepehrmansourie, M. A. Zolfigol, R. Karamian and S. H. M. Farida, *New J. Chem.*, 2018, **42**, 14308–14317.
59 M. Rajabi-Salek, M. A. Zolfigol and M. Zarei, *Res. Chem. Intermed.*, 2018, **44**, 5255–5269.
60 E. Noroozizadeh, A. R. Moosavi-Zare, M. A. Zolfigol, M. Zarei, R. Karamian, M. Asadbegy, S. Yari and S. H. M. Farida, *J. Iran. Chem. Soc.*, 2018, **15**, 471–481.
61 A. R. Moosavi-Zare, M. A. Zolfigol, M. Zarei, A. Zare and V. Khakyzadeh, *J. Mol. Liq.*, 2015, **211**, 373–380.
62 M. A. Zolfigol, *Tetrahedron*, 2001, **57**, 9509–9511.
63 M. Zarei, M. A. Zolfigol, A. R. Moosavi-Zare, E. Noroozizadeh and S. Rostamnia, *ChemistrySelect*, 2018, **3**, 12144–12149.